

EXPERIMENTAL DEFORMATION OF DEUTERATED ICE IN 3D AND 2D: IDENTIFICATION OF GRAIN-SCALE PROCESSES

CHRISTOPHER J.L. WILSON¹, VLADIMIR LUZIN², SANDRA PIAZOLO³,
MARK PETERNELL⁴ & DANIEL HAMMES⁴

¹School of Earth, Atmosphere and Environment, Monash University, Victoria 3800, Australia

²Australian Nuclear Science and Technology Organisation (ANSTO), Lucas Heights, NSW, 2232, Australia

³Department of Earth and Planetary Sciences, Macquarie University, NSW 2109, Australia

⁴Institute of Geosciences, University of Mainz, 55128 Mainz, Germany

Correspondence: Chris.Wilson@monash.edu

ABSTRACT: Major polar ice sheets and ice caps experience cycles of variable flow during different glacial periods and as a response to past warming. The rate and localisation of deformation inside an ice body controls the evolution of ice microstructure and crystallographic fabric. This is critical for interpreting proxy signals for climate change, with deformation overprinting and disrupting stratigraphy deep under ice caps due to the nature of the flow. The final crystallographic fabric in polar ice sheets provides a record of deformation history, which in turn controls the flow properties of ice during further deformation and affects geophysical sensing of ice sheets. For example, identification of layering in ice sheets, using seismic or ice radar techniques, is attributed to grain size changes and fabric variations. Such information has been used to provide information on climate state and its changes over time, and as the Fourth Intergovernmental Panel on Climate Change (IPCC) Report (Solomon et al. 2007) points out there is currently still a lack of understanding of internal ice-sheet dynamics. To answer this we have recently conducted experiments at the Australian Nuclear Science and Technology Organisation (ANSTO) to collect fully quantitative microstructural data from polycrystalline heavy water (D₂O) ice deformed in a dynamic regime. The ice and temperature (-7°C) chosen for this study is used as a direct analogue for deforming natural-water ice as it offers a unique opportunity to link grain size and texture evolution in natural ice at -10°C. Results show a dynamic system where steady-state rheology is not necessarily coupled to microstructural and crystallographic fabric stability. This link needs to be taken into account to improve ice-mass-deformation modelling critical for climate change predictions.

Keywords: deuterated ice, neutron diffraction, deformation, microstructure, texture

ICE SHEETS AND RHEOLOGY

Ice-sheet flow is through a combination of localised internal plastic deformation and sliding at the base of the ice. The internal deformation is strongly dependent on temperature, strain-rate, crystal orientation, and defect structure (Duval et al. 1983; Schulson & Duval, 2009). Here we present experiments using deuterated ice (D₂O), as this allows quantitative in situ, neutron-diffraction texture analysis while studying a material with the same crystal structure, mechanical properties and deformation behaviour as H₂O ice (Wilson et al. 2014). Low attenuation of neutrons in D₂O allows large bulk-sample analysis insensitive to boundary effects, improved texture quality and grain statistics over conventional techniques (Wenk 1986; Piazzolo et al. 2008; Wilson & Peternell 2011) and quantitative measurements with short time resolution at strain-rates relevant to the flow of glaciers and ice-sheets. These results will then be compared with 2-D experiments undertaken on a fabric analyser (Wilson et al. 2003; Wilson et al. 2007) and their application to polar ice sheets.

NEUTRON DIFFRACTION 3D EXPERIMENTS

The neutron diffractometer KOWARI at ANSTO (Kirstein et al. 2009) was used to measure textures and grain size evolution in polycrystalline deuterated ice samples (Piazzolo et al. 2013). Experiments were performed at -7°C, a temperature equivalent to -10°C for naturally deforming ice sheets and glaciers. Each neutron diffraction experiment consisted of two major steps. First, diffraction patterns were collected over a range of different directions with respect to the sample by rotating the load frame and sample away from the compression axis (ω in Figure 1). The range over which ω was varied was $\pm 35^\circ$. In this way we could continuously monitor the textural (Matthies et al. 1987) and grain size characteristics during the deformation of a deuterated ice sample (Figure 1). Figure 2b is a typical picture of the integrated and normalised absolute intensities for the (002) diffraction peak recorded in partial pole figures from fast ($1 \times 10^{-5} \text{ s}^{-1}$), medium ($2.5 \times 10^{-6} \text{ s}^{-1}$) to slow ($6 \times 10^{-7} \text{ s}^{-1}$) strain-rate experiments. Between 5–10% deformation there is a rapid increase in intensity, with the greatest being associated with the slowest deformation (Figure 2b).

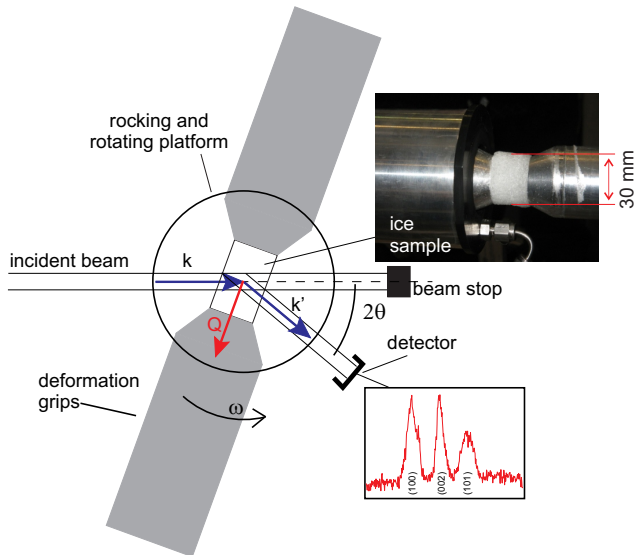


Figure 1: Schematic illustration of the Kowari instrument configuration for 3D neutron diffraction and texture analysis. Insert shows deformed ice sample, from an initial sample that had a diameter ~ 2.5 cm, length ~ 3.2 – 4.0 cm.

Figure 3 shows the stress-strain relationship, in which we identified four distinct stages in the deformational behaviour of ice measured by mechanical means. For all strain-rates initial deformation is characterised by a steep increase in stress (Stage I). During Stage II, stresses reach their peak at strains of $\sim 2\%$ accompanied by subsequent weakening. This is followed by a 15–35% decay in strength (Stage III). At higher strains, the flow stress is nearly steady state (Stage IV). Weakening of the aggregate occurs from the peak stress in Stage II to a steady-state flow stress reached at strain of $\sim 10\%$ (medium strain-rate) and $\sim 20\%$ (slow strain-rate). The strain ranges of Stage I ($0\% < \text{strain} < 1.5\%$) and Stage II ($1.5\% < \text{strain} < 3.5\%$) are identical for all experiments while the boundary between Stages III and IV occurs at progressively increasing strain with increasing strain-rate.

The neutron diffraction patterns also provided information about the evolution of mean grain size as a function of change in strain-rate and strain (Figure 3b). For medium and high strain-rates grain size decrease

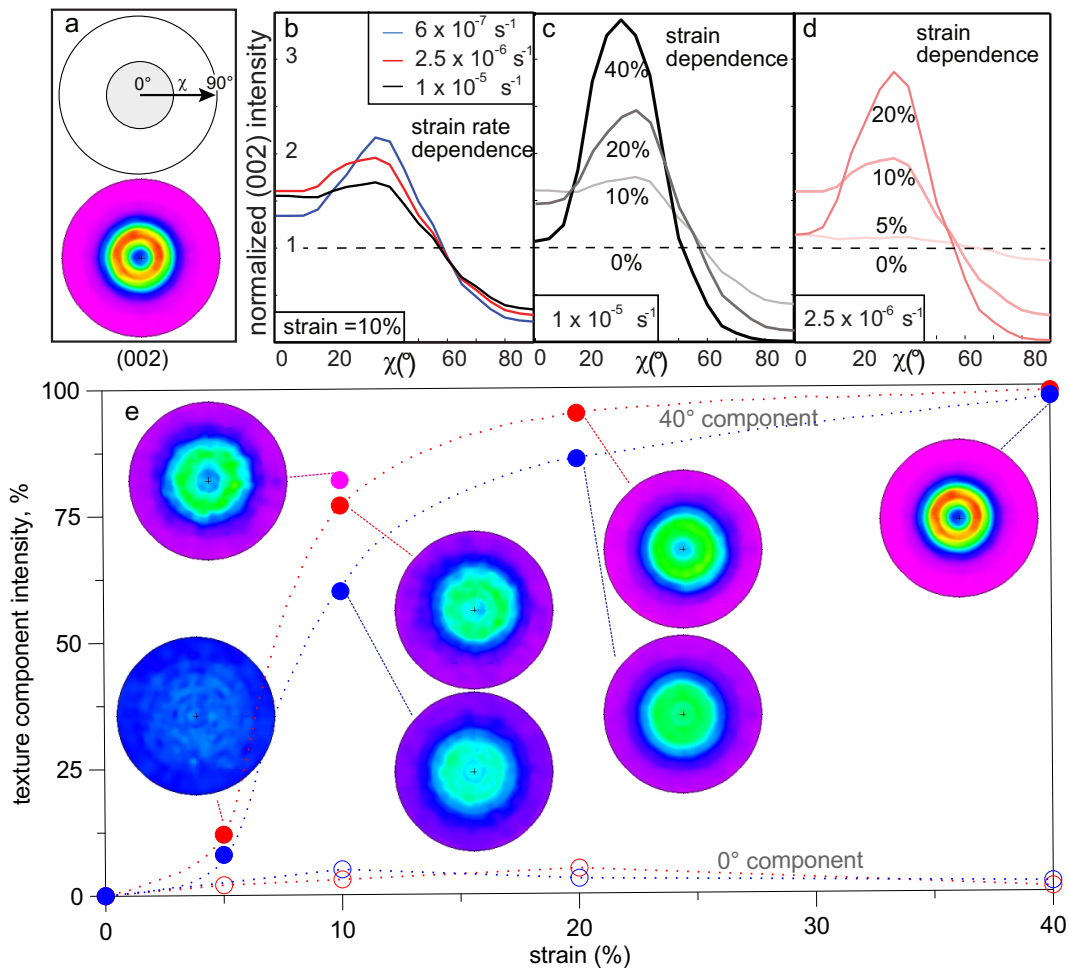


Figure 2: Texture analysis from 3D neutron diffraction experiments. (a) Partial pole figure (top) and full pole figure data (bottom) are cylindrically symmetric about the shortening axis. This allows all full pole figures (e) to be presented in one-dimensional sections (b–d) showing (b) the strain-rate [$6 \times 10^{-7} \text{ s}^{-1}$ (slow), $2.5 \times 10^{-6} \text{ s}^{-1}$ (medium) and $1 \times 10^{-5} \text{ s}^{-1}$ (fast)] or (c) and (d) strain dependence. In the figure only the (002) pole figure data are presented. Textures from all samples were analysed in terms of fibre texture components (standard distributions over the surface of a sphere similar to a Gaussian distribution) and presented quantitatively in (e).

relatively slowly during Stage I, whereas in a slow strain-rate experiment the grain size remains constant within the error range. During stage II there is a reduction in grain size for all strain-rates. Within stage III the rate of grain size reduction decreases for the medium and fast strain-rate series. In contrast, with a slow strain-rate the grain size reaches a minimum at strains $\sim 4\%$, stays constant until $\sim 6\%$ and increases until there is 10% shortening. During stage IV grain sizes show a stabilisation with a slight grain size increase in the slow strain-rate experiments.

In the second step, each sample was removed from the load frame and mounted in a device for orienting the sample (a two-circle Eulerian cradle equipped with a cooling device and kept below -80°C). This allowed us to produce complete pole figures (Figure 2) for the three diffraction peaks corresponding to the indices (100), (002) and (101), to fully characterise the texture of the samples. During the initial stage of deformation (Stage I) the textural development is dominated by dislocation movement and slip on the basal plane (Wilson et al. 2014), resulting in the

rotation of the c -axes parallel to the shortening axis and an increase in the intensity of (002) (Figure 2a). However, basal slip can only accommodate a small proportion of the deformation, thus stresses increase markedly (Figure 3a), until there is activation of pyramidal and prismatic slip (Piazolo et al. 2013). New grain nucleation rates appear to significantly increase during Stage II (Figure 3b). Once the rate of nucleation is increased, grain sizes decrease rapidly for all strain-rates (Stage II, Figure 3b). Once, the volume of new, soft grains is significant the ice starts to weaken (Stage III, Figure 3b). In high-strain experiments (Figures 2c–d), nucleation originating from highly hardened ice results in grains of high orientation spread, many not favourable for the employed deformation conditions, keeping the ice still relatively hard. This is in contrast to slow strain-rate experiments (Figure 3b), where grain boundary migration results in the early selection of soft grains. Hence, the ice is in a strain-softening situation and the integrated (002) intensity is higher in slow strain-rate experiments with a small circle at $\sim 30^\circ$ from the compression axis (Figure 2).

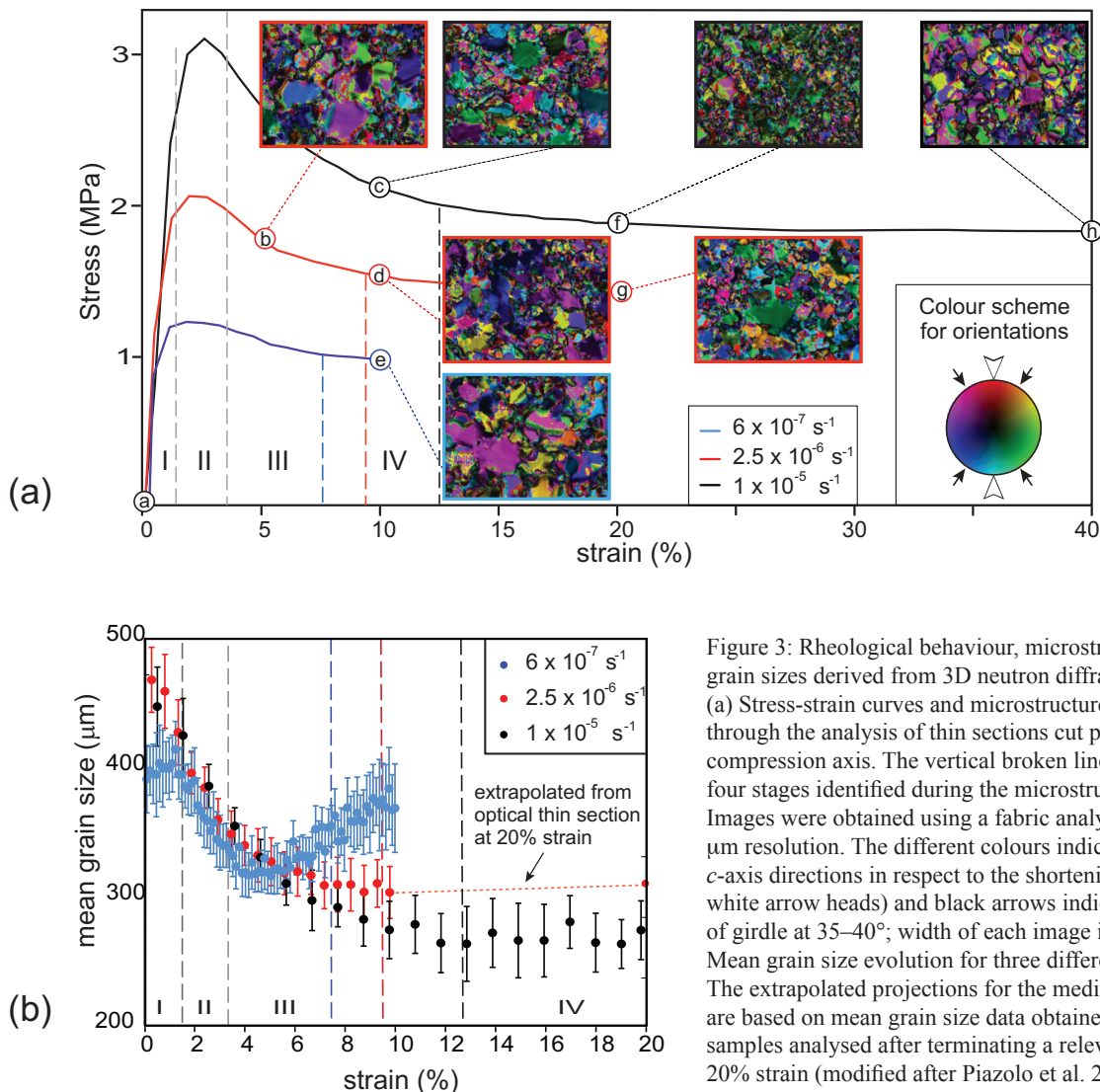


Figure 3: Rheological behaviour, microstructures and mean grain sizes derived from 3D neutron diffraction analysis. (a) Stress-strain curves and microstructures obtained through the analysis of thin sections cut parallel to the compression axis. The vertical broken lines indicate the four stages identified during the microstructural evolution. Images were obtained using a fabric analyser with a $5 \mu\text{m}$ resolution. The different colours indicate different c -axis directions in respect to the shortening axis (large white arrow heads) and black arrows indicate the position of girdle at $35-40^\circ$; width of each image is 4.8 mm . (b) Mean grain size evolution for three different strain-rates. The extrapolated projections for the medium strain-rate are based on mean grain size data obtained optically from samples analysed after terminating a relevant experiment at 20% strain (modified after Piazolo et al. 2013).

FABRIC ANALYSER 2D EXPERIMENTS

Continuous and synchronous recording of microstructure and crystal c -axis orientations have been performed on thin wafers (~ 120 μm thick), by the use of an automated fabric analyser (Wilson et al. 2007; Wilson et al. 2014). We were able to analyse grain microstructural and crystal orientation development during a constant strain-rate (Figure 4a) and compare these results with observations where strain-rate varied over time between long intervals and short intervals of deformation (Table 1). The starting material was polycrystalline deuterated ice, which had a mean grain size of ~ 300 μm and random c -axis preferred orientations (Figure 4). Differential strain-rates were achieved by changing the rate at which the piston was advanced into the sample (Paternell et al. 2011).

After deforming the ice at a constant strain-rate, the mean grain size reduced to 230 μm during a stage of new grain nucleation accompanied by grain boundary migration. The initial random crystal-orientation by end of experiment had stabilised between a single-point maximum and a girdle distribution (Figure 5). In the long-interval strain-rate cycling experiment, the eigenvector E1 is rotated approximately parallel to the shortening direction, and the crystal-orientation pattern becomes an intermediate girdle-cluster-type crystal-orientation pattern

(Figure 5). The short-interval strain-rate cycle experiment shows a fine grained microstructure (120 μm), with crystal orientations almost unchanged and near isotropic (Figure 5).

Similar crystal orientation patterns are recognised at polar ice divides, characterised as random c -axis patterns, indicating isotropic ice near the surface, and as a small circle at around 30° from the compression axis and is supported by compressional deformation experiments (Jacka & Li 2000). In contrast, the short-interval cycles do not develop any identifiable textural pattern (Figure 5) as in the basal parts of an ice sheet (Tison et al. 1994).

CONCLUSIONS

The experiments we report demonstrate that dramatic changes in grain size and texture development can be the direct result of either a constant or cyclicity of events in the flow of an ice mass. This has important ramifications on ice-sheet models that are commonly based on the assumption that the ice is isotropic at the ice-sheet surface, with the continuous development (continuum model) of a vertical single-maximum c -axis orientation with increasing depth (De La Chapelle et al. 1998). On this basis our experimental observations contradict the continuum model for crystal-size evolution in polar ice sheets (Ng & Jacka 2014). There is a limiting grain size associated with any

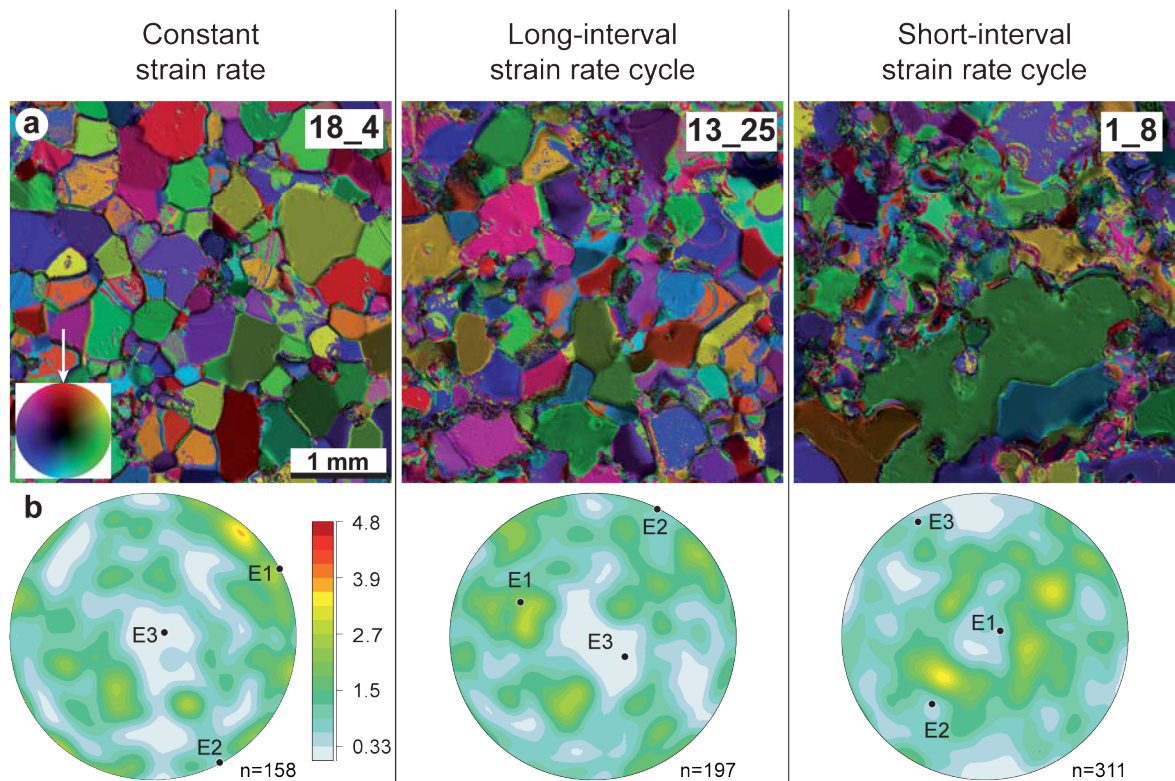


Figure 4: Initial microstructure and crystal c -axis directions in 2D fabric analyser experiments. The colour wheel image indicates c -axis directions in respect to the vertical shortening axis (white arrow) and eigenvectors E1, E2, E3 of the c -axis orientation tensor. n = number of c -axes measured and colour-scale bar indicates contour intervals.

Table 1: List of 2D fabric analyser experiments discussed in text.

Sample	Type of experiment	T (°C) deformation	Time (h) deformation	Strain-rate ($\times 10^{-6}$ 1/s)	Incremental shortening (%)	Strain (%)
18_4	constant strain-rate	-7	21	2.5	0.06	19.2
13_25	long-interval strain-rate cycle	-7	16	10.2 1.45	0.3–0.04	17.71
1_8	short-interval strain-rate cycle	-7	22	1.9 2.8	0.05–0.07	18.61

repetitive short-cycle variations in strain-rate on grain growth; this does not have a strong effect on the resulting grain size, but changes the path of grain size development. The experimental results also imply that a short-interval strain-rate history may have a significant ‘memory effect’ upon grain size and fabric and this will probably influence the flow stress within the ice mass. This experimental approach highlights the highly dynamic behaviour of ice where grain size, texture and microstructure may change continuously while the rheological response is near steady state. This suggests that grain size or texture alone is insufficient to infer rheological responses in natural ice. Indeed, microstructural evolution controls many physical properties of the ice (Alley et al. 1986), and identification of layering in ice sheets using seismic or ice radar techniques (Fujita et al. 2000; Eisen et al. 2007) is attributed to grain size changes and texture variations. Such information has

been used to provide information on climate state and its changes over time (palaeoclimates) and as the Fourth IPCC Assessment Report (Solomon et al. 2007) points out, there is currently still a lack of understanding of internal structure and dynamics in ice sheets.

Acknowledgements

This work was supported by the Australian Nuclear Science and Technology Organisation (ANSTO) during projects 1702, 2701 and 2910. The technical support from the ANSTO staff is gratefully acknowledged. S.P. was supported by the Australian Research Council (Project FT110100070 and DP120102). M.P. and D.M.H. were financially supported by the Centre for Computational Sciences in Mainz, Germany (SRFN). We thank Trevor Finlayson for a constructive review.

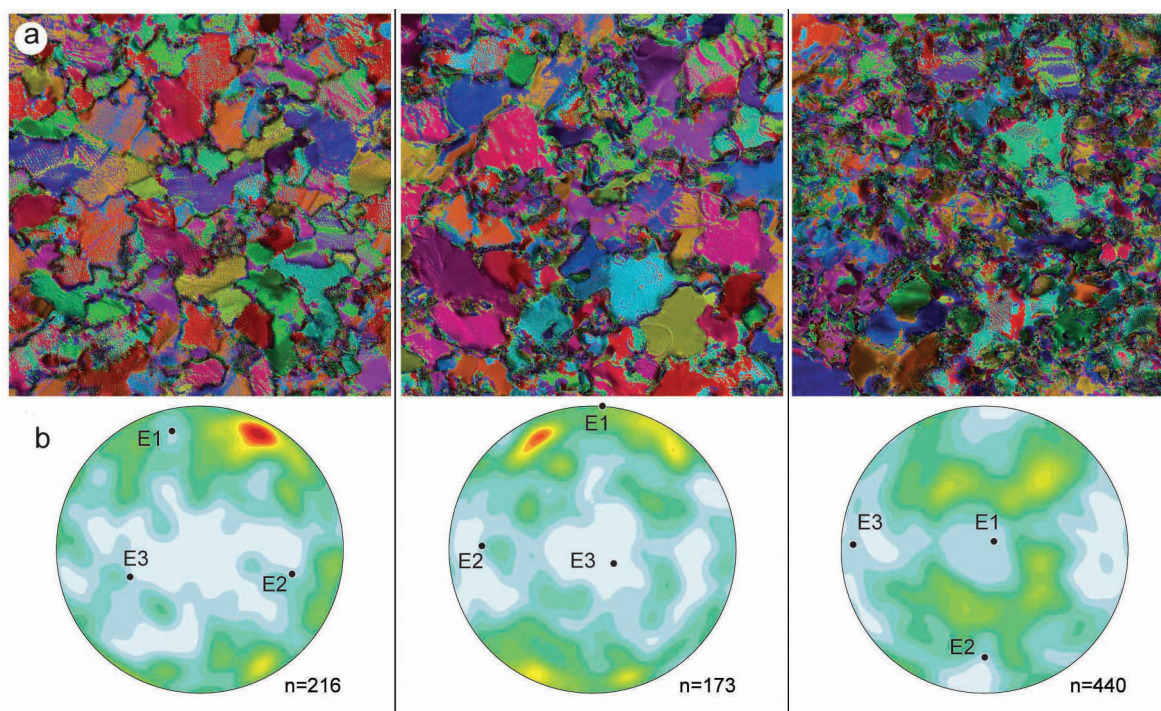


Figure 5: Final microstructures and textures after vertical shortening and annealing in 2D experiments. (a) Final microstructure after deformation (row 1). (b) Crystal *c*-axis directions for grains after deformation (row 2). Eigenvectors E1, E2, E3 are indicated. *n* = number of *c*-axes measured and colour-scale bar indicates contour intervals.

References

- Alley, R.B., Perepezko, J.H. & Bentley, C.R., 1986. Grain growth in polar ice: I. theory. *Journal of Glaciology* 32: 415–424.
- De La Chapelle, S., Castelnau, O., Lipenkov, V. & Duval, P., 1998. Dynamic recrystallization and texture development in ice as revealed by the study of deep ice cores in Antarctica and Greenland. *Journal of Geophysical Research* 103: 5091–5105.
- Duval, P., Ashby, M.F. & Anderman, I., 1983. Rate-controlling processes in the creep of polycrystalline ice. *Journal of Physical Chemistry* 87: 4066–4074.
- Eisen, O., Hamann, I., Kipfstuhl, S., Steinhage, D. & Wilhelms, F., 2007. Direct evidence for continuous radar reflector originating from changes in crystal-orientation fabric. *Cryosphere* 1: 1–10.
- Fujita, S., Matsuoka, T., Ishida, T., Matsuoka, K. & Mae, S., 2000. A summary of the complex dielectric permittivity of ice in the megahertz range and its applications for radar sounding of polar ice sheets. In *Physics of Ice Core Records I*, T. Hondoh, ed. Hokkaido University Press, Sapporo, pp. 185–212.
- Jacka, T.H. & Li, J., 2000. Flow rates and crystal orientation fabrics in compression of polycrystalline ice at low temperature and stresses. In *Physics of Ice Core Records I*, T. Hondoh, ed. Hokkaido University Press, Sapporo, pp. 83–113.
- Kirstein, O., Luzin, V., & Garbe, U., 2009. The strain-scanning diffractometer Kowari. *Neutron News* 20: 34–36.
- Matthies, S., Vinel, G.W. & Helming, K., 1987. *Standard Distributions in Texture Analysis*. Akademie-Verlag, Berlin.
- Ng, F. & Jacka, T.H., 2014. A model of crystal-size evolution in polar ice masses. *Journal of Glaciology* 60: 463–477.
- Peternell, M., Russell-Head, D.S. & Wilson, C.J.L., 2011. A technique for recording polycrystalline structure and orientation during *in situ* deformation cycles of rock analogues using an automated fabric analyser. *Journal of Microscopy* 242: 181–188.
- Piazo, S., Montagnat, M. & Blackford, J.R., 2008. Sub-structure characterization of experimentally and naturally deformed ice using cryo-EBSD. *Journal of Microscopy* 230: 509–519.
- Piazo, S., Wilson, C.J.L., Luzin, V., Brouzet, C. & Peternell, M., 2013. Dynamics of ice mass deformation: linking processes to rheology, texture and microstructure. *G-Cubed* 14: 4185–4194.
- Schulson, E.M. & Duval, P., 2009. *Creep and Fracture of Ice*. Cambridge University Press, Cambridge.
- Solomon, S., Qin, D., Manning, M., Chen, Z., Marquis, M., Averyt, K.B., Tignor, M. & Miller, H.L., 2007. *Contribution of Working Group I to the Fourth Assessment Report of the Intergovernmental Panel on Climate Change*, Cambridge University Press, New York.
- Tison, J.-L., Thorsteinsson, T., Lorrain, R.D. & Kipfstuhl, J., 1994. Origin and development of textures and fabrics in basal ice at Summit, Central Greenland. *Earth and Planetary Science Letters* 125: 421–437.
- Wenk, H.-R. 1986. *An Introduction to Modern Texture Analysis*. Academic Press, London.
- Wilson, C.J.L. & Peternell, M.A., 2011. Evaluating ice fabrics using fabric analyser techniques in Sørtdal Glacier, East Antarctica. *Journal of Glaciology* 57: 881–894.
- Wilson, C.J.L., Russell-Head, D.S. & Sim, H.M., 2003. The application of an automated fabric analyser system to the textural evolution of folded ice layers in shear zones. *Annals Glaciology* 37: 7–17.
- Wilson, C.J.L., Russell-Head, D.S., Kunze, K. & Viola, G., 2007. The analysis of quartz *c*-axis fabrics using a modified optical microscope. *Journal of Microscopy* 227: 30–41.
- Wilson, C.J.L., Peternell, M., Piazo, S., & Luzin, V., 2014. Microstructure and fabric development in ice: lessons learned from *in situ* experiments and implications for understanding rock evolution. *Journal of Structural Geology* 61: 50–77.